Mast, R. F., "Microscopic Behavior of Foam in Porous Media," paper SPE 3997, Society of Petroleum Engineers of AIME, 6200 North Central Expressway, Dallas, Tex. 75206 (1972).
Melrose, J. C., "Wettability as Related to Capillary Action in Porous Media," *Soc. Petrol. Eng. J.*, **5**, 259 (1965).
Miller, E. E., and R. D. Miller, "Physical Theory for Capillary Flow Phenomena," *J. Appl. Phys.*, **27**, 324 (1956).
Minssieux, L., "Oil Displacement by Foams in Relation to Their Physical Properties in Porous Media," *J. Petrol. Technol.*, 100 (Jan., 1974).
Morrow, N. R., "The Effects of Surface Roughness on Contact Angle with Special Reference to Petroleum Recovery," *J. Can. Pet. Technol.*, 42 (Oct.-Dec., 1975).
Oh, S. G., and J. C. Slattery, "Interfacial Tension Required for Significant Displacement of Residual Oil," *Soc. Petrol. Eng. J.*, **19** (1979).
Payatakes, A. C., C. Tien, and R. M. Turian, "A New Model for Granular Porous Media: Part I. Model Formulation," *AIChE J.*, **19**, 58 (1973).
Raza, S. H., "Foam in Porous Media: Characteristics and Potential Applications," *Soc. Petrol. Eng. J.*, **10**, 328 (1970).
Slattery, J. C., "Interfacial Effects in the Entrapment and Displacement of Residual Oil," *AIChE J.*, **20**, 1145 (1974).
Yarnold, G. D., "The Motion of a Mercury Index in a Capillary Tube," *Proc. Phys. Soc. London*, **50**, 540 (1938).

Manuscript received May 16, 1977; revision received April 6, and accepted October 5, 1978.

The Dynamic Behavior of a CSTR: Some Comparisons of Theory and Experiment

R. A. SCHMITZ

and

R. R. BAUTZ

Department of Chemical Engineering
University of Illinois
Urbana, Illinois 61801

and

W. H. RAY

and

A. UPPAL

Department of Chemical Engineering
State University of New York at Buffalo
Buffalo, New York 14214

Mathematical methods employed recently in a theoretical study by Uppal et al. (1974) are applied to the second-order homogeneous reaction between sodium thiosulfate and hydrogen peroxide and are combined with experimental investigations of that reaction using a nonadiabatic continuous stirred tank reactor (CSTR). A complete portrayal of the expected behavior of that reaction system is presented in parameter space. Some new experimental studies of reactor instabilities are presented and linked to that portrayal. Close agreement is shown between theoretical predictions and experimental data.

SCOPE

Recent publications by Uppal et al. (1974, 1976) have summarized, added to, and given order to the plethora of prior theoretical information on the classical problem regarding steady state multiplicity, stability, and oscillations in a continuous stirred tank reactor (CSTR) for a first-order, exothermic Arrhenius reaction. Publications of experimental investigations of these phenomena in homogeneous reaction systems had appeared, though they were sparse at that time. Among these were experiments by Vetjtasa and Schmitz (1970) and Chang and Schmitz (1975a,b) which employed the second-order liquid phase reaction between sodium thiosulfate and hydrogen peroxide. The present investigation employs this reaction system and amounts to a union between experimental studies and the analytical methods employed by Uppal et al. The general intention was to enhance the significance of both lines of research. Specifically, the objectives of the work were to elucidate completely the possible behavioral traits for the thiosulfate-peroxide reaction system, which has proved to be useful for laboratory tests and demonstrations of CSTR behavioral characteristics, and to relate these findings to previously reported experimental results; to examine the feasibility of using the existing experimental facility for conducting experimental tests of behavior predicted theoretically but not previously observed; and to conduct, with the guidance of theoretical results, feasible laboratory tests.

Correspondence concerning this paper should be addressed to R. A. Schmitz. R. R. Bautz is with St. Regis Paper Company, West Nyack, New York. W. H. Ray is at the University of Wisconsin, Department of Chemical Engineering, Madison, Wisconsin. A. Uppal is with Xerox of Canada, Mississauga, Ontario, Canada.

0001-1541-79-2125-0289-$01.15.

CONCLUSIONS AND SIGNIFICANCE

The principal result of the theoretical portion of this work was a delineation in parameter space of the various predicted types of steady state and oscillatory situations for the thiosulfate-peroxide reaction. (To some extent, these theoretical results apply generally to second-order Arrhenius reactions in a CSTR, but certain parameter values were fixed to correspond to those of the experimental facility at hand.) The results were used to design experiments aimed directly at studying situations in which there exist three steady states for a given set of parameters, only one being stable to small perturbations, but there being no sustained oscillations (limit cycles). Experimental investigations into this type apparently have not been conducted previously for homogeneous reactions. The experiments showed, as predicted theoretically, that one of the unstable states (the highest conversion state) could be stabilized by deliberately increasing the heat capacity of the reactor. When the increased capacity was removed, small oscillations set in, grew in amplitude, and eventually led to steady operation at the only stable state (a low conversion state). In the experimental tests, the excess heat capacity was provided by a pool of water held in an annular space surrounding the reactor wall. Experimentally obtained steady states, both stable and unstable, and phase plots are shown to be in very good agreement with theoretical predictions. As it turned out, other interesting predicted situations, not previously studied experimentally, could not be investigated either because they called for parameter values beyond those attainable in the experimental facility or because their existence was confined to impractically small regions in parameter space.

The research reported in this paper is significant because the bringing of the methods of theoretical analysis used by Uppal et al. (1974) to bear on a real reaction system and the close coupling of laboratory experiments to the theory result in a better understanding and appreciation of the steady state and dynamic complexities of the CSTR. Furthermore, the demonstrated role of extraneous heat capacities in determining the stability or instability of certain steady states has practical significance in the scale-up process in which information gained from small reactors is used to predict the performance of large commercial ones. The former usually have large relative extraneous capacities, while the latter ordinarily have negligibly small ones. The operating state predicted for the large reactor may be unattainable owing to unanticipated intrinsic instabilities.

Among the recent developments in the area of chemical reactor stability have been experimental studies of the steady state and dynamic behavior of exothermic liquid phase reactions in the CSTR (Vejtasa and Schmitz, 1970; Chang and Schmitz, 1975*a*, *b*), and an overall theory which forms the capstone of a lengthy history of theoretical investigations into the behavior of these reactors (Uppal et al., 1974, 1976). The aforementioned experiments employed the second-order liquid phase reaction between sodium thiosulfate and hydrogen peroxide to investigate the existence of multiple steady states and of sustained oscillatory states. The theoretical work of Uppal et al. (1974, 1976) applied stability and bifurcation analysis as well as topological arguments to a first-order reaction kinetic model. The principal result of that work was a summary, in terms of regions in reactor parameter space, which characterized the possible types of CSTR behavior with special emphasis on the multiplicity and stability of steady states and the emergence, disappearance, and stability of periodic orbits (sustained oscillatory states; limit cycles). [Additional references to both experimental and theoretical work in this area may be found in a recent review paper (Schmitz, 1975).]

The present study represents a merger of these two lines of investigation. Among the results of the work are an elucidation of the theoretically predicted behavior for the thiosulfate-peroxide reaction in a CSTR, the attainment in the laboratory of a type of instability which apparently has not previously been reported for homogeneous reactions, and the confronting of theoretical model predictions with experimental fact.

MATHEMATICAL MODEL

It has been shown in a previous study (Chang and Schmitz, 1975*a*) that the reaction rate between sodium thiosulfate and hydrogen peroxide in aqueous solution is accurately described by a second-order Arrhenius type of expression, first order with respect to each reactant.* A preexponential factor k_o of 1.63×10^{10} l/mole s, an activation energy E_a of 16 190 cal/gmole, and a molar stoichiometric ratio of peroxide to thiosulfate of 2 were reported in that study. The stoichiometric equation for the reaction is

$$Na_2S_2O_3 + 2\ H_2O_2 \rightarrow \text{Products}$$

The basic species and energy balance equations were presented in earlier work of Chang and Schmitz (1975*a*) and can be put in the following dimensionless form:

$$\frac{dx_1}{d\theta} = -x_1 + Da\,[(b - x_1)(1 - x_1)] \exp\left(\frac{\gamma x_2}{\gamma + x_2}\right) \tag{1}$$

* As indicated in the study by Chang and Schmitz (1975*a*), the kinetics of this reaction are apparently dependent on the ranges of temperature and concentrations employed as well as on the nature of the reagent solutions. The present study was essentially confined to the same conditions as described in the cited reference.

TABLE 1. NUMERICAL VALUES FOR PARAMETERS AND CONSTANTS

A_C	500 cm²
$C_{A,F}$	0.97 mole/l
$C_{B,F}$	1.46 mole/l
$-\Delta H/\rho C_p$	146.4 l°C/gmole $Na_2S_2O_3$
T_C	260°K
T_F	273°K
$\frac{1}{U}$	$\frac{19}{1+0.021T}+\frac{208}{q_C^{0.8}}$ (T in °C; q_C in ml/s; U in $\frac{\text{cal}}{\text{cm}^2\,\text{s}\,^\circ\text{C}}$)
V	980 ml
ρC_p	1.0 cal/cm³ °C
$\rho_c C_{pc}$	0.842 cal/cm³ °C

$$\frac{dx_2}{d\theta} = -\alpha x_2 + Da\hat{B}\,[(b-x_1)(1-x_1)]\exp\left(\frac{\gamma x_2}{\gamma+x_2}\right)+\hat{\beta}x_{2C} \quad (2)$$

The basic system of equations also contains a species balance on thiosulfate, but the concentration C_A of thiosulfate can be related stoichiometrically to x_1 by the relationship $2(C_A - C_{A,F})/C_{B,F} = x_1$. According to arguments by Chang and Schmitz (1975*a*), this relationship may be assumed to hold for both the steady and unsteady states.

The parameter groups $\hat{B}$ and $\hat{\beta}$ in Equation (2) are analogous to groups B and β defined by Uppal et al. (1974), except that here they are modified by the factor $1/(1+\epsilon)$ which accounts for extraneous heat capacities. This same factor gives rise to the new parameter α which did not appear in the model of Uppal et al. The extraneous heat capacities are those of materials other than, but in thermal contact with, the reacting fluid, such as reactor walls, etc. Since the factor appears homogeneously on the right-hand side of Equation (2), it has no effect on the steady state. Its effect on the transient state and stability was discussed in the paper by Chang and Schmitz (1975*a*).

Parameter values which apply to the experimental part of this study are listed in Table 1. These fix the values of b and γ at 1.33 and 29.8, respectively. The remaining parameter groups α, $\hat{B}$, $\hat{\beta}x_{2C}$, and Da are manipulatable by changes in the feed and coolant flow rates and by changes in ϵ. Such experimentally related matters receive further attention later, but the handling of the factor H, and thus of the groups α and $\hat{\beta}x_{2C}$, requires some mention at this point. The factor H is effectively a heat transfer coefficient defined such that the product $H(T - T_c)$ represents the total rate of heat loss to the coolant. Taking T_c to be the inlet temperature of a liquid which flows through submerged cooling coils at a volumetric rate q_c, one can use energy balances to derive the following expression for H in terms of an overall heat transfer coefficient U:

$$H = q_c\rho_c C_{pc}\left[1-\exp\left(\frac{-UA_c}{q_c\rho_c C_{pc}}\right)\right] \quad (3)$$

In the experimental system, U was found to be a function of reactor temperature, as well as of coolant flow rate, and was correlated by the expression given in Table 1. Yet in the theoretical analysis to follow, the product $H\tau$ is treated as a constant; hence α and $\hat{\beta}x_{2C}$ are treated as independent parameters. This is justifiable, but further explanation is best handled in a later section.

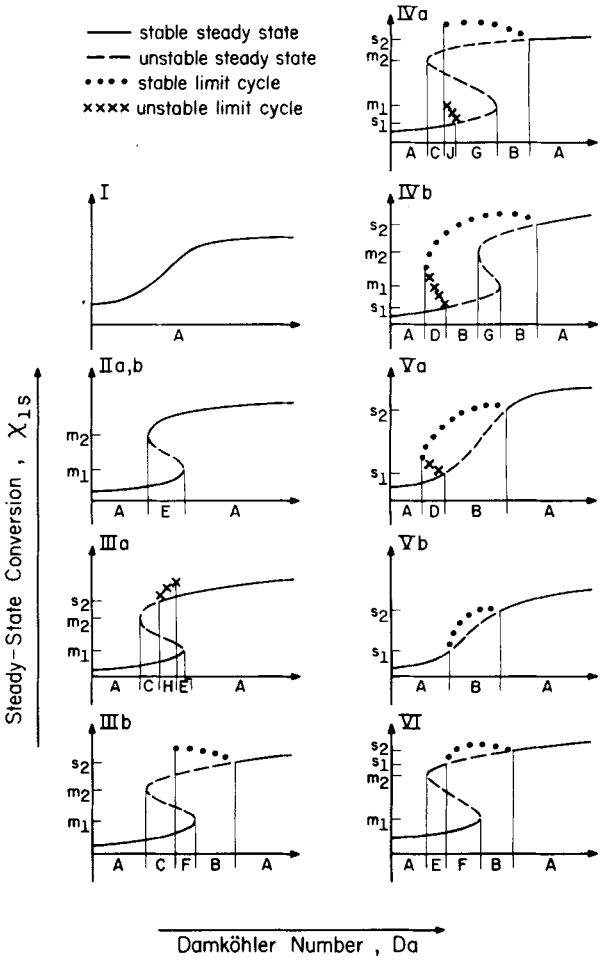

Fig. 1. Sketches showing the possible steady state and oscillatory characteristics and types of phase plots for the CSTR.

THEORY

Classification of the Reactor Behavior

The qualitative features of the dynamic behavior of the CSTR for a second-order reaction are similar to those for the first-order case, the analysis for which was presented in detail by Uppal et al. (1974, 1976). For this reason, the presentation here is concise. Mathematical derivations and proofs are omitted [a general reference is the paper by Uppal et al. (1974)], but sufficient description is retained so that the additional analytical complexities which come to fore with higher-order reactions are made known and that the connection between theoretical and experimental aspects for the particular reaction system at hand is apparent.

For the steady state condition, Equations (1) and (2) yield the following relationship for the Damköhler number Da:

$$Da = \frac{x_{1S}}{(b-x_{1S})(1-x_{1S})}\exp\frac{-(\hat{B}x_{1S}+\hat{\beta}x_{2C})}{\gamma\alpha+\hat{B}x_{1S}+\hat{\beta}x_{2C}} \quad (4)$$

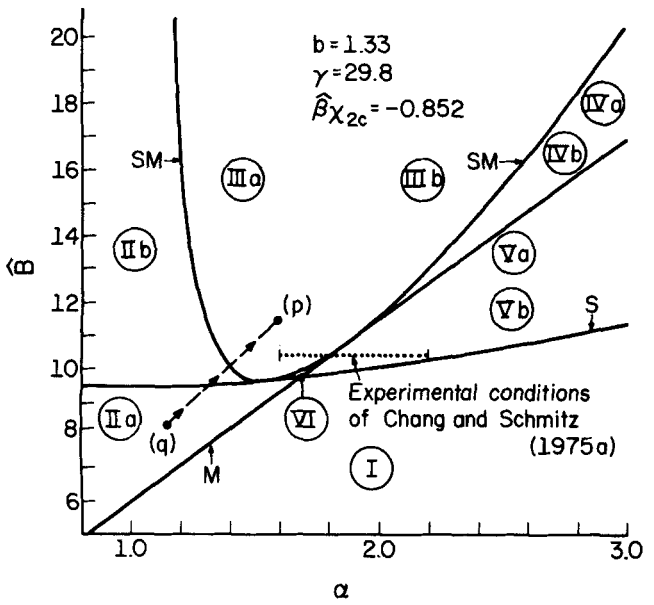

Fig. 2. Computed results in the $\alpha,\hat{B}$ plane for the thiosulfate-peroxide reaction with $\hat{\beta}x_{2C} = -0.852$.

As pointed out by Uppal et al. (1974), the necessary and sufficient condition for the reactor to have multiple steady states for a fixed set of parameters is that the derivative dDa/dx_{1S} be negative over some range of x_{1S} values (with $0 < x_{1S} < 1$). Accordingly, setting of this derivative equal to zero and utilizing Equation (4) for the differentiation leads to the following equation whose roots x_{1S} are the values of the conversion at which multiplicity begins (or ends):

$$x_{1S}^4 + \left[2\left(\frac{\alpha}{\hat{B}}\gamma + \frac{\hat{\beta}}{\hat{B}}x_{2C}\right) + \frac{\alpha}{\hat{B}}\gamma^2\right]x_{1S}^3 + \left[\left(\frac{\alpha}{\hat{B}}\gamma + \frac{\hat{\beta}}{\hat{B}}x_{2C}\right)^2 - b - (1+b)\frac{\alpha}{\hat{B}}\gamma^2\right]x_{1S}^2 + \left[\frac{b\alpha}{\hat{B}}\gamma^2 - 2b\left(\frac{\alpha}{\hat{B}}\gamma + \frac{\hat{\beta}}{\hat{B}}x_{2C}\right)\right]x_{1S} - b\left(\frac{\alpha}{\hat{B}}\gamma + \frac{\hat{\beta}}{\hat{B}}x_{2C}\right)^2 = 0 \tag{5}$$

As in the case of first-order kinetics, it can be shown that Equation (5) has either zero or two real roots for $0 < x_{1S} < 1$. The roots for the latter case are denoted here by m_1 and m_2 which correspond to the points indicated on the ordinate of some of the sketches in Figure 1.

Equation (5) serves as the defining equation for a bifurcation surface in the parameter space of α, $\hat{B}$, b, γ, and $\hat{\beta}x_{2C}$. The surface separates the space into two domains, one throughout which unique steady states are guaranteed and the other throughout which multiple states (that is, multiple solutions for x_{1S}) exist over a range of values of Da. Following the approach adopted by Uppal et al. (1974), we represent this notion graphically and conveniently here by considering that three parameters b, γ, and $\hat{\beta}x_{2C}$ are fixed. The surface then is a bifurcation curve in a α, $\hat{B}$ plane. Such curves, called hereafter M curves, are shown in that plane for two sets of the fixed parameters in Figures 2 and 3. Notice that the second-order reaction gives rise to a quartic equation in x_{1S} for the bifurcation condition [Equation (5)], while the analogous equation for a first-order reaction was quadratic (Uppal et al., 1974). Computations of the M curves in Figures 2 and 3, therefore, required a numerical search procedure amounting essentially to seeking the locus of points in the α, $\hat{B}$ plane which separates the portion of the plane throughout which all roots x_{1S} of Equation (5) are complex from the portion throughout which the two real roots m_1 and m_2 exist.

Additional characteristics of the reactor behavior may be depicted in the same parameter plane by inquiring into the local stability of the steady states. The usual analysis for local stability proceeds via Liapunov's first method and utilizes the following linearized form of Equations (1) and (2):

$$\frac{dy}{dt} = \mathbf{A}\,y$$

where

$$y = \begin{bmatrix} x_1 - x_{1S} \\ x_2 - x_{2S} \end{bmatrix}$$

$$\mathbf{A} = \begin{bmatrix} -1 - \dfrac{x_{1S}(1+b-2x_{1S})}{(b-x_{1S})(1-x_{1S})} & \dfrac{x_{1S}}{\left(1+\dfrac{x_{2S}}{\gamma}\right)^2} \\ -\dfrac{\hat{B}\,x_{1S}(1+b-2x_{1S})}{(b-x_{1S})(1-x_{1S})} & -\alpha + \dfrac{\hat{B}x_{1S}}{\left(1+\dfrac{x_{2S}}{\gamma}\right)^2} \end{bmatrix} \tag{6}$$

The well-known necessary and sufficient conditions for local stability are that the determinant of the coefficient matrix $\mathbf{A}$ be positive and that the trace of $\mathbf{A}$ be negative. The first of these leads to the condition that the value of x_{1S} must be such that $m_1 > x_{1S} > m_2$ for stability. Regarding the second condition, vanishing of the trace of $\mathbf{A}$ defines the value or values of x_{1S} at which bifurcations to periodic solutions (limit cycles) occur, provided that the value or values are not in the range $m_1 < x_{1S} < m_2$. Setting the trace of $\mathbf{A}$ equal to zero and making substitutions for x_{2S} in terms of x_{1S} from Equations (1) and (2) and subsequently for Da from Equation (4) leads to the following quartic polynomial in x_{1S}:

$$\left(\frac{\alpha-1}{\alpha^2}\right)^2 x_{1S}^4 + \left[\frac{2(\alpha-1)\hat{\beta}x_{2C}}{\alpha^2\hat{B}} + \frac{2(\alpha-1)\gamma}{\alpha\hat{B}} - \frac{1+b}{\alpha} - \frac{\gamma^2}{\hat{B}}\right]x_{1S}^3 + \left[\frac{(\alpha-1)\gamma^2}{\hat{B}^2} + \frac{b(1+\alpha)}{\alpha^2} + \frac{1+b}{\hat{B}}\gamma^2\right.$$

$$- (1-\alpha)\left(\frac{\hat{\beta}x_{2C}}{\hat{B}\alpha}\right)^2$$

$$- \frac{2(1+b)\gamma}{\hat{B}} - \frac{2(1-\alpha)\gamma\hat{\beta}x_{2C}}{\alpha\hat{B}^2}$$

$$- \frac{2(1+b)\hat{\beta}x_{2C}}{\alpha\hat{B}}\Big]x_{1S}^2$$

$$+\Big[\frac{2b(1+\alpha)\gamma}{\alpha\hat{B}} - \frac{(1+b)}{\alpha}\left(\frac{\hat{\beta}x_{2C}}{\hat{B}}\right)^2$$

$$- \frac{2(1+b)\gamma\hat{\beta}x_{2C}}{\hat{B}^2}$$

$$+ \frac{2b(1+\alpha)\hat{\beta}x_{2C}}{\alpha^2\hat{B}} - \frac{b\gamma^2}{\hat{B}}$$

$$- \frac{\alpha(1+b)\gamma^2}{\hat{B}^2}\Big]x_{1S}$$

$$+ b(1+\alpha)\left(\frac{\hat{\beta}x_{2C}}{\alpha\hat{B}}\right)^2 + \frac{2b(1+\alpha)\hat{\beta}x_{2C}}{\alpha\hat{B}^2}$$

$$+ b(1+\alpha)\gamma^2/\hat{B}^2 = 0 \qquad (7)$$

It can be shown that there exist, at most, two real roots for x_{1S} to Equation (7) for $0 < x_{1S} < 1$. Examples of these are depicted by the symbols s_1 and/or s_2 on the ordinate of some of the sketches in Figure 1. As indicated in those sketches, a locus of points, schematically representing the peak values of x_{1S} on limit cycles, emanates from points corresponding to conversion levels s_1 and s_2 on the steady state curves.

As was the case with Equation (5), Equation (7) gives rise to a bifurcation curve, called the S curve, in the parameter plane of Figures 2 and 3. The computation of the S curve involved a numerical search for the locus of those points in the $\alpha, \hat{B}$ plane for which real positive values of x_{1S} first appeared as roots to Equation (7). As it turns out, points lying above the S curve lead to a violation of the trace condition and therefore to a possibility of limit cycles. Limit cycles are assured over some range of *Da* values when one of the following conditions is met: no real roots m_1 and m_2 exist from Equation (5) while at the same time Equation (7) yields two real roots s_1 and s_2, as, for example, in the sketches labeled Va and Vb in Figure 1, or the real roots s_1 and s_2 exist from Equation (7), but not both have values between m_1 and m_2. Examples of the latter possibilities are shown in the sketches labeled IIIa, IIIb, IVa, IVb, and VI in Figure 1. A boundary curve which along with the M and S curves defines the various regions in the $\alpha, \hat{B}$ plane is the SM curve shown in Figures 2 and 3. The SM curves in those figures were obtained by locating numerically those points at which a root m_1 or m_2 from Equation (5) had the same value as a root s_1 or s_2 from Equation (7). Clearly, the problem of locating those curves is not a trivial computational task. Even more formidable would be computations of curves which separate the pattern of sketch IIIa from that of IIIb, the pattern of sketch IVa from that of IVb, and the pattern of Va from that of Vb. We felt that the computations of these curves were not warranted here, but considerable discussion of them, and example computations regarding them for the first-order case, may be found in the paper by Uppal et al. (1974).

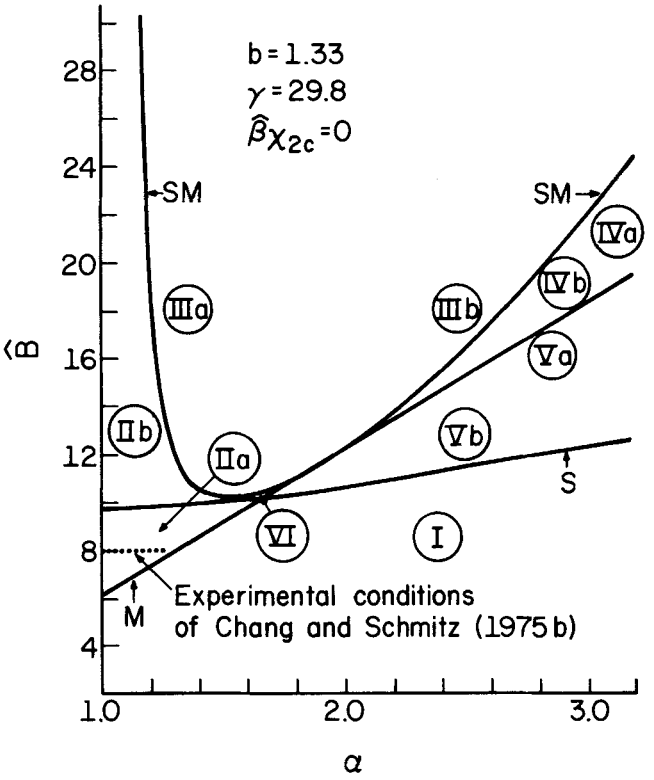

Fig. 3. Computed results in the $\alpha,\hat{B}$ plane for the thiosulfate-peroxide reaction with $\hat{\beta}x_{2C} = 0$.

The complete description of the reactor behavior requires, in addition to Figures 1, 2, and 3, a depiction of the various possible types of phase plane portraits. Uppal et al. (1974) show that altogether there are nine types of portraits and label them A, B, ..., H, and J. (The possible types are displayed in Figure 6 of that reference.) There are no new types arising for the case of second-order kinetics, and to save space here, we do not show these various portraits. Notice, however, that the abscissas of Figure 1 are segmented, each segment bearing a label corresponding to one of the nine types. For convenience and clarity in subsequent discussion, we occasionally denote situations of interest by their region in the parameter space and by their phase plane type. For example, situations of particular interest in experiments described below are those in regions IIIa and IIIb of type C; situations in which three values of x_{1S} exist, only one is stable, and there are no limit cycles.

Relation to the Experimental System

Previous experimental studies with the peroxide-thiosulfate system in a CSTR have yielded situations of types A, B, and E. For one of those studies (Chang and Schmitz, 1975*b*), the locus of operating conditions covered is marked by the horizontal dotted line segment in Figure 3. As indicated by that segment, experiments were in region IIa; hence, situations studied were of types A and E. (We have neglected the value of ϵ in locating the dotted segment in Figure 3. The value of that parameter is difficult to fix in any case. Furthermore, we should point out that this study focused on the stabilization of the intermediate unstable states by means of automatic

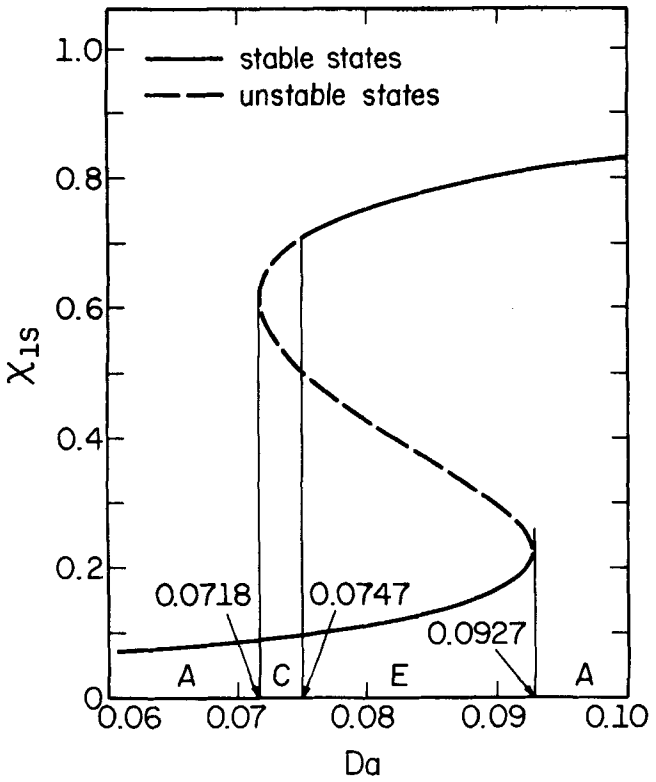

Fig. 4. Predicted steady state conversion curve for the experimental system for point (p) in Figure 2.

feedback control. The dotted segment in Figure 3 represents the uncontrolled reactor; the control strategy cannot be represented in that figure.)

The experiments of Vejtasa and Schmitz (1970) were with an adiabatic reactor. Therefore, their conditions covered a vertical line segment in Figure 3 at $\alpha = 1$ (or actually to the left of $\alpha = 1$ if a nonzero value of ϵ is considered). As can be seen from Figure 3, only regions I, IIa, and IIb are accessible under those conditions. Accordingly, only phase plots of types A and E were observed in the experiments of Vejtasa and Schmitz.

Another series of experiments reported by Chang and Schmitz (1975*a*) cannot be located accurately relative to the curves in either of the parameter planes of Figures 1 or 2 because the value of $\hat{\beta}x_{2C}$, a fixed parameter in those planes, was not held constant. The dotted line segment in Figure 2 shows the value of $\hat{B}$ and the range of values of α for those experiments (again, we have neglected the value of ϵ), but the value of the parameter group $\hat{\beta}x_{2C}$ varied from about -1.70 to -0.852. However, the curves in the $\alpha, \hat{B}$ plane are not very sensitive to that parameter group, as can be deduced from a comparison of Figures 2 and 3. As indicated by the dotted segment of Figure 2, the experimental study of Chang and Schmitz (1975*a*) straddled regions III and V. The study focused on limit cycle behavior and consequently displayed situations only of type A in region III and of types A and B in region Vb.

The type of experiment suggested by the theoretical results described in earlier sections of this paper and the type planned in the present work are ones in which the parameter groups α, $\hat{B}$, b, $\hat{\beta}x_{2C}$, and γ are all held constant, and the Damköhler number *Da* is varied. In this manner, a single point is defined in the α, $\hat{B}$ plane. By varying the value of *Da*, one would then expect to observe the various types of steady state and oscillatory patterns predicted in Figure 1 for the region corresponding to that particular point. In conducting such an experiment, however, one must contend with the following difficulty. The only convenient experimental parameter in the Damköhler number is the residence time τ or, more specifically, the feed flow rate. However, $\hat{\beta}$, and hence α and $\hat{\beta}x_{2C}$ also depend on τ. Thus, the experimental plan demands that H be manipulated in such a way that the product $H\tau$, and hence $\hat{\beta}$, remains constant as *Da* is varied.*

The approach in the experimental part of this work was to fix $\hat{\beta}x_{2C}$ at a value of -0.852 which corresponds to a value of $\hat{\beta}$ of 0.60. (Values of b and γ were fixed at 1.33 and 29.8, respectively, as stated earlier.) The intention was to use the theoretical results of Figure 2 to guide the selection of experimental conditions so as to lead to types of states that have not previously been observed for this reaction system. Thus, the primary interest, insofar as experiments were concerned, was in situations of types C, D, F, G, H, and J which might be found in regions IIIa, IIIb, IVa, IVb, Va, and VI of Figure 2. We carried out a large number of computations and simulations covering all of these regions, the essential result being that region IIIa was the only experimentally feasible region to explore for behavior not previously observed and that situations of type C were the only new ones to expect. As shown in Figure 1, for situations of type C, there exist three steady states, the high and intermediate conversion states being unstable. All trajectories in the phase plane approach the only stable state; there are no limit cycles (Uppal et al., 1974). Computations revealed that the experimentally accessible portion of the parameter plane in Figure 2 was toward the lower left. The main limitations in extending studies to larger values of $\hat{B}$ and α were those of the cooling system capacity in the present laboratory facility along with the lower and upper limits on steady state and feed temperatures of about 0° and 100°C. Region VI was experimentally feasible but was simply too small to attempt to reach in the laboratory. Furthermore, computations that were carried out in the accessible portions of the regions of interest showed that with the exception of type C in region III, the new types of phase plots being sought existed over such narrow ranges of values of *Da* that they would be unattainable experimentally, including types F and H in regions IIIa and IIIb.

It should be clear that these results regarding the attainability of certain types of behavior are due to experimental limitations and to this particular reaction system. They do not necessarily have any bearing on the general significance of the various situations depicted in Figures 1 to 3.

As a result of the computations and simulations, a single point ($\alpha = 1.6$, $\hat{B} = 11.5$) was selected in region III for the experimental work described in the following section. For this point, indicated by point (p) in Figure 2, the

* For the coupling of experimental work with theory, it would obviously be of advantage to have the parameter groups redefined so that the residence time affects only a single parameter. This approach makes the theoretical delineation of regions in parameter space and of the nature of steady states more difficult, but it has been adopted in a recent study by Uppal et al. (1976) for a first-order kinetic model. Analogous computations for a second-order reaction would be quite cumbersome and were not attempted in our work.

predicted steady state conversion x_{1S} vs. Da is shown in Figure 4. As indicated in that figure, situations of types A, C, and E are predicted. The range of Da values for types F or H is so small as to be practically nonexistent. Notice that type C is on a narrow range of Da values as well, but it is an experimentally feasible range.*

As mentioned earlier, phase plots of type C have not previously been observed for this reaction system or, for that matter, for any homogeneous reaction to our knowledge. This type, however, has been reported for the catalytic oxidation of hydrogen on a platinum catalyst in a recirculating reactor by Horak and Jiracek (1972). It should be mentioned here also that situations of type F have been observed for the isothermal platinum catalyzed oxidation of carbon monoxide in gradientless reactors (Hugo and Jakubith, 1972; McCarthy et al., 1975; Plichta, 1976; Schmitz, 1975). References to studies of these phenomena and related ones are contained in a recent review paper by Sheintuch and Schmitz (1977).

Finally, attention is called to the dashed line segment directed from point (q) to point (p) in Figure 2. That segment is intended to show schematically the path that is followed by α and $\hat{B}$ as ϵ is decreased to a value of zero at point (p). Recall that ϵ accounts for the presence of extraneous heat capacities and that it has no effect whatsoever on the steady state. Therefore, in the experimental system, situations of type E in region II may be converted to those of type C in region III when extraneous heat capacities are made sufficiently small. The reverse, of course, is true if the capacities are made large. This is an important point in the experimental study of type C phase plots as described below. One should realize that changing ϵ also changes the value of $\hat{\beta}x_{2C}$, one of the parameter groups held constant in Figure 2, and therefore also changes the locations of the curves in Figure 2. However, as pointed out earlier, those curves are not very sensitive to changes in $\hat{\beta}x_{2C}$, and the essential conclusion that region II is approached as ϵ increases can be proven in general for points in the α, $\hat{B}$ plane lying above the M curve.

EXPERIMENTS

Equipment and Procedures

The laboratory facility and the general experimental procedures used for the present study have been described previously (Chang and Schmitz, 1975*a*); only the more salient features and important modifications are described here. The reactor, similar in most respects to the one designated as reactor A in the paper by Chang and Schmitz (1975*a*), was cylindrical in shape, constructed from type 304 stainless steel foil with a wall thickness of 0.002 in. and a bottom thickness of 0.04 in. The reactor had a void volume for the reacting mixture of 980 ml. Heat removal was to a brine solution which flowed through a stainless steel coil submerged in the reacting mixture.

An important modification made in the experimental system for the present study was the addition of a cylindrical Plexiglas housing which surrounded the reactor wall and created an annular gap of about ½ in. between the housing and the wall. The usual procedure during experiments was to allow the reactor to reach a steady state with the gap filled with about 400 ml of water. The purpose of the water was to provide an extraneous heat capacity of such magnitude that the high conversion states in phase plots of type C would be stabilized. The housing was equipped with a drain tube at the bottom so that the water could be removed conveniently. Removing the water would decrease the value of ϵ, presumably to a point where a state that had been stable with the water present would become unstable. Thus, adding and removing water in an experiment would cause movement of the operating point in the α, $\hat{B}$ plane of Figure 2 along the dashed line, approaching point (p) when the water was entirely removed.

To ensure good thermal contact between the water and the reactor contents, air was sparged through the annular space. In addition, the housing was insulated from the surroundings so that there were no appreciable heat losses at steady state from the reactor to the water. The water thus served simply to provide an extra heat capacity; it had no effect on the steady state of the reactor. With 400 ml of water in the annular gap, the value of ϵ was about 0.4. Accordingly, the initial value of α and $\hat{B}$ corresponded roughly to point (q) on the dashed line in Figure 2.

Three copper constantan thermocouples were located in the reactor contents, and another was in the annular water. Temperature measurements from these thermocouples differed by less than 0.5° at a steady state.

The experimental system was interfaced to an IBM-1800 digital computer. The role of the computer was to sample and store temperature data from the reactor as

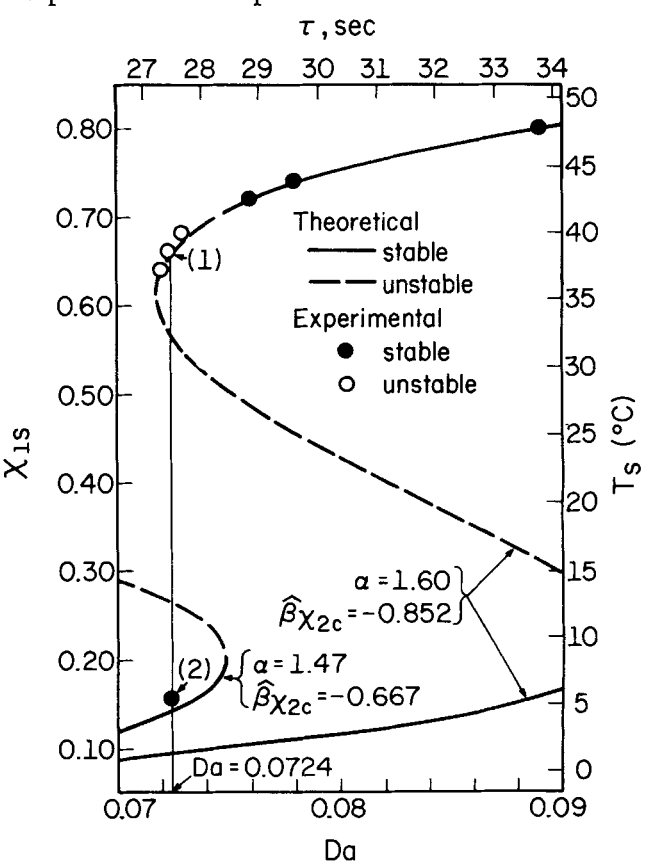

Fig. 5. Theoretical and experimental results.

* All theoretical results discussed in connection with the remaining figures in this paper, beginning with Figure 4, incorporate a value of ϵ of 0.015 in the appropriate parameter groups. This value seemed reasonable in light of previous experiments by Chang and Schmitz (1975*a*). Theoretical results in remaining figures also take into account the temperature dependence of the factor H in $\hat{\beta}$ and hence in α and $\hat{\beta}x_{2C}$. It seems that neither of these effects leads to a noteworthy change in the steady state curves, in stability characteristics, or in the various regions in the parameter plane and the types of phase plots. We found the effects to be significant, however, in the quantitative description of the unsteady state. Therefore, they were retained in all computer programs used directly in conjunction with the experiments.

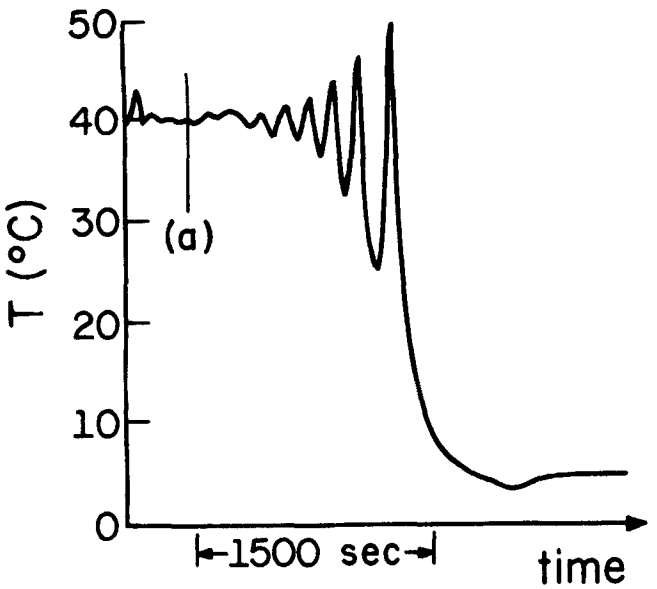

Fig. 6. Temperature transient following sudden reduction, at point (a), of system heat capacity with $Da = 0.0724$.

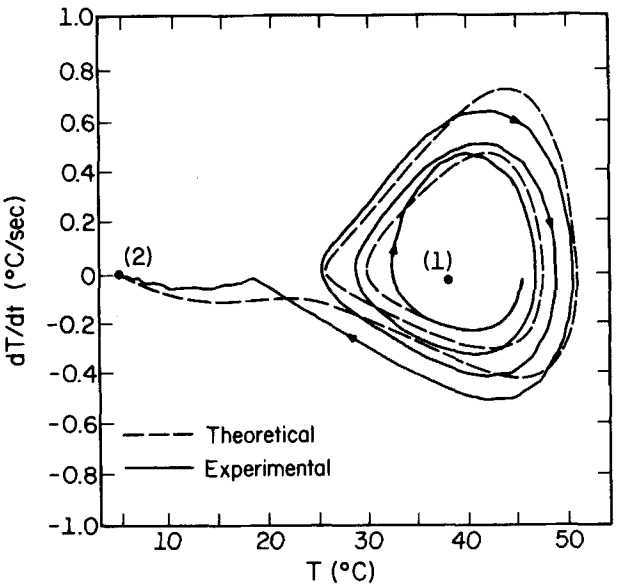

Fig. 7. Phase plot for the temperature transient of Figure 6. Points (1) and (2) correspond to those indicated for $Da = 0.0724$ in Figure 5.

well as from the inlet and outlet coolant line at time intervals of 2 s. The coolant flow rate was also sampled (as a voltage signal from a differential pressure transmitter on an orifice) and later used along with the temperatures in energy balance equations to compute and correlate the heat transfer coefficient. (The resulting correlation in terms of reactor temperature and coolant flow rate is that given in Table 1.) At the end of an experiment, a plotter, also on line with the digital computer, was used to obtain temperature-time plots and phase plane trajectories of dT/dt vs. T. For the latter plots, the instantaneous temperature derivative was computed from the stored reactor temperature data by means of a five-point smoothing algorithm.

As mentioned earlier, the experiments were conducted in such a way that $\hat{\beta}$ was maintained constant at 0.60, and the Damköhler number was manipulated by changing the feed flow rate. The range of Damköhler number of interest was from about 0.07 to 0.09. This range called for residence time changes from 26.4 to about 33.9 s, which in turn called for coolant flow rate changes from about 70 to 40 ml/s in order to maintain $\hat{\beta}$ constant. In the course of the experiments, then, the feed flow rate (or residence time) was dictated by the desired value of Da. The value of H was calculated to give $\hat{\beta} = 0.6$, and the coolant flow was set according to the value of q_c given by Equation (4), with U taken from the correlation in Table 1. For these purposes, the temperature used in the computation of U was the theoretically predicted steady state temperature.

Results

Experiments were carried out at six different values of Da. For three of these, the high conversion state was predicted to be stable, and for the others it was predicted to be unstable. The resulting steady states are shown along with theoretical predictions of their stability and types of phase plots in Figure 5. As indicated by the data shown in Figure 5, there was excellent agreement between theoretical and experimental results with regard both to the steady state values and to their stability. The steady state conversion shown on the left ordinate in Figure 5 was not measured directly in the experiments; it was computed from steady state equations using the measured reactor temperature T_s. Note that values of T_s are given on the right ordinate in Figure 5, and the residence time is shown on the top abscissa.

The three states determined to be unstable in the experiments with water removed from the jacket were at Da values of 0.0720, 0.0724, and 0.0730, which corresponded to residence times of 26.4, 27.3, and 27.5 s, respectively. [The estimated experimental error in the residence time values could be kept as low as $\pm$ 0.1 s with careful attention to rotameter settings. In fact, the portion of the steady state curve of interest is quite sensitive to all parameters. Feed concentrations were prepared to specified values with a maximum deviation of 1%, and coolant flow rates were accurate to $\pm$ 0.5 ml/s. As an indication of the precision attained in the data presented here, point (1) in Figure 5 was reproduced on three separate occasions with no appreciable deviation in the steady state temperature.] The data points shown for these states in Figure 5 were obtained with the extraneous water present in the jacket surrounding the reactor wall, and in this case these steady states were stable. When the water was removed the steady states become unstable, and natural disturbances led to the onset of small amplitude oscillations in the reactor temperature. The oscillations grew in amplitude for several periods until the eventually led to an asymptotic approach to a stable, low conversion state. This transient temperature, which effectively is a consequence of making a sudden change from point (q) to point (p) in Figure 3, is shown for $Da = 0.0724$ in Figure 6. In this case, the state prior to the removal of the jacket water corresponded to point (1) in Figure 5 and the final state to point (2) in that figure. Points (1) and (2) in Figure 5 lie on separate curves because of the manner in which the experiments with transient behavior were conducted. [The curve through point (1), in fact, is the curve shown in Figure 4.] No attempt was made to hold H, hence $\hat{\beta}$, constant during the unsteady state. Instead, the coolant flow rate q_c was held constant at its value at the high conversion state, for example, at its value corresponding to point (1) in Figure 5 for the case of $Da = 0.0724$. As

the temperature changed in the unsteady state, U changed (and H, $\hat{\beta}$, α, and $\hat{\beta}x_{2C}$ as well) because of its temperature dependence. Thus, the final state, that is point (2) in Figure 5 for the case of $Da = 0.0724$, was at a different value of α and $\hat{\beta}x_{2C}$ as indicated in the figure. An adjustment in q_c to reset U to its original value would presumably have moved point (2) onto the same curve as point (1).

Figure 7 shows both the experimental and the simulated transient responses in the phase plane of dT/dt vs. T. In order to permit a meaningful comparison between the two, the initial point on the simulated response was taken to be identical to a point on the experimental curve at a time somewhat after the onset of oscillations. The two curves in Figure 7 show very good agreement in both a qualitative and quantitative sense.

The other two unstable cases depicted in Figure 5 gave very similar results. None of them led to sustained oscillations. Furthermore, experiments showed that small perturbations from those states indicated as being stable in Figure 5 for Da values of 0.076, 0.078, and 0.089 decayed regardless of whether or not the extraneous water was present.

As concluding remarks, we emphasize again the excellent agreement between theory and experiment (an affirmation principally of the perfect mixing model and of the accuracy of model constants, including reaction kinetic constants) and the combination of a theoretical analysis and an experimental technique which enabled us to demonstrate a type of reactor instability and dynamic behavior not previously reported for this type of system. Furthermore, the role of extraneous heat capacities in reactor stability considerations was clearly demonstrated. This role may indeed be important in practical scale-up problems because certain imminent instabilities in large commercial reactors (where extraneous capacities are relatively small) may be nonexistent in pilot plant or bench scale counterparts (where extraneous capacities are relatively large).

ACKNOWLEDGMENT

This work received financial support through grants from the National Science Foundation (ENG 74-21094) and from the Gulf Oil Foundation. Most of the chemicals used in the experiments were donated by the Shell Chemical Company. A. Uppal and W. H. Ray conducted research for this paper while they were guests of Professor E. D. Gilles at the Institut für Systemdynamik and Regelungstechnik of the University of Stuttgart. W. H. Ray is indebted to the Guggenheim Foundation for financial support during that time.

NOTATION

$\mathbf{A}$ = coefficient matrix defined in Equation (6)
A_c = heat transfer area
b = dimensionless parameter group, $2C_{A,F}/C_{B,F}$
$\hat{B}$ = dimensionless parameter group, $(-\Delta H)\, C_{B,F}\, \gamma / [2\rho C_p T_F(1+\epsilon)]$
C_A, C_B = concentrations of sodium thiosulfate and hydrogen peroxide, respectively
C_p, C_{pc}, C_{pm} = heat capacities of the reacting mixture, coolant, and extraneous reactor materials, respectively
Da = Damköhler number for second-order reaction, $\tau k(T_F) C_{B,F}$
E = activation energy
H = heat transfer function defined in Equation (3)
ΔH = enthalpy of reaction
$k(T)$ = reaction velocity factor, $k_o \exp(-E/R_gT)$
k_o = preexponential factor in Arrhenius rate law
m = mass of extraneous reactor material
m_1, m_2 = real positive roots (between zero and unity) of Equation (5)
q, q_c = volumetric flow rates of reacting mixture and coolant, respectively
R_g = universal gas constant
s_1, s_2 = real positive roots (between zero and unity) of Equation (7)
t = time
T = reactor temperature
T_C = inlet coolant temperature
U = overall heat transfer coefficient
V = reactor volume
x_1 = fractional conversion of peroxide, $(C_{B,F} - C_B)/C_{B,F}$
x_2 = dimensionless temperature, $(T - T_F)\, \gamma/T_F$
x_{2C} = dimensionless inlet coolant temperature, $(T_C - T_F)\, \gamma/T_F$
$\mathbf{y}$ = vector of perturbation variables defined in Equation (6)

Greek Letters

α = dimensionless parameter group, $\hat{\beta} + 1/(1+\epsilon)$
$\hat{\beta}$ = dimensionless parameter group, $H\tau/\rho C_p V(1+\epsilon)$
γ = dimensionless activation energy, E/R_gT_F
ϵ = ratio of heat capacity of solids to heat capacity of reacting fluid, $mC_{pm}/V\rho C_p$
ρ, ρ_C = densities of reacting mixture and coolant, respectively
θ = dimensionless time, t/τ
τ = residence time, V/q

Subscripts

F = feed state
S = steady state

LITERATURE CITED

Chang, M., and R. A. Schmitz, "An Experimental Study of Oscillatory States in a Stirred Reactor," *Chem. Eng. Sci.*, 30, 21 (1975*a*).

———, "Feedback Control of Unstable States in a Laboratory Reactor," *ib.d.*, 30, 837 (1975*b*).

Horak, J., and F. Jiracek, "A Study of the Dynamic Behaviour of Catalytic Flow Reactors," *5th European/2nd International Symposium on Chemical Reaction Engineering*, p. B8-1, Amsterdam (1972).

Hugo, P., and M. Jakubith, "Dynamisches Verhalten und Kinetik der Kohlenmonoxid-Oxidation am Platin-Katalysator," *Chem-Ing.-Tek.*, 44, 383 (1972).

McCarthy, E., J. Zahradnik, G. C. Kuczynski, and J. J. Carberry, "Some Unique Aspects of CO Oxidation on Supported Pt," *J. Catal.*, 39, 29 (1975).

Plichta, R. T., "Oscillations in the Oxidation of Carbon Monoxide on an Unsupported Platinum Catalyst," Ph.D. thesis, Univ. Ill., Urbana (1976).

Schmitz, R. A., "Multiplicity, Stability, and Sensitivity of States in Chemically Reacting Systems—A Review," *Advan. Chem. Ser.*, 148, 156 (1975).

Sheintuch, M., and R. A. Schmitz, "Oscillations in Catalytic Reactions," *Catal. Rev.-Sci. Eng.*, 15, 107 (1977).

Uppal, A., W. H. Ray, and A. B. Poore, "On the Dynamic Behavior of Continuous Stirred Tank Reactors," *Chem. Eng. Sci.*, 29, 967 (1974).

———, "The Classification of the Dynamic Behavior of Continuous Stirred Tank Reactors—Influence of Residence Time," *ibid.*, 31, 205 (1976).

Vejtasa, S. A., and R. A. Schmitz, "An Experimental Study of Steady-State Multiplicity and Stability in an Adiabatic Stirred Reactor," *AIChE J.*, 16, 410 (1970).

Manuscript received March 13, 1978; revision received August 25 and accepted September 6, 1978.